Received February 26, 2020, accepted March 10, 2020, date of publication March 16, 2020, date of current version April 20, 2020.

Digital Object Identifier 10.1109/ACCESS.2020.2981050

Broadband Circularly Polarized Cross-Dipole Antenna With Multiple Modes

LEI WANG, WEN-XIAO FANG, WEI-HENG SHAO, BIN YAO, YUN HUANG, AND YUN-FEI EN
The Science and Technology on Reliability Physics and Application of Electronic Component Laboratory, China Electronic Product Reliability and Environmental Testing Research Institute, Guangzhou 510610, China

Corresponding authors: Wen-Xiao Fang (fangwx@ceprei.com) and Yun-Fei En (enyf@ceprei.com)

ABSTRACT A broadband circularly polarized (CP) cross-dipole antenna with multiple modes is proposed. The antenna is composed of two pairs of crossed strip dipoles as driven elements, four square-slot patches, and four corner-truncated patches as parasitic elements. A pair of vacant-quarter printed rings is used as sequential phase feeding structure to generate a CP mode, which connect to crossed strip dipoles. By using these coupled rotated elements, multiple CP modes can be stimulated to satisfy the need of broadband CP radiation. In addition, four shorted square metal columns are also introduced in the antenna design to generate an additional CP resonance. A verified prototype was fabricated and measured in this paper. The measured results demonstrate the proposed antenna features wideband CP characteristics with a wide impedance bandwidth (IBW) of 95.5% (0.92-2.60 GHz) and a broad axial-ratio bandwidth (ARBW) of 94.4% (0.95-2.65 GHz).

INDEX TERMS Broadband, circularly polarized (CP), cross-dipoles, parasitic elements, sequentially rotated configuration.

I. INTRODUCTION

Owing to the outstanding features of suppressing multipath effects and mitigating polarization mismatch compared with linearly polarized antennas, circularly polarized (CP) antennas have been increasingly attractive in modern communication systems, for example various navigation satellite system (GPS/BDS/GLONASS), radio frequency identification (RFID), and wireless local area network (WLAN). Due to these communication systems usually operate in different frequency bands, multiple antennas will be inevitably installed together to simultaneously satisfy these application demand, which increases the complexity and push up cost of system. Therefore, wideband CP antenna will be a potential candidate for implement multiple bandwidth coverage.

In past years, all kinds of broadband CP antennas have been designed by utilizing different radiated structures [1]–[20]. Such as utilizing higher resonator order modes [1] or introducing additional dielectric resonators [2], using external hybrid couplers [3], dielectric polarizers [4] or artificial magnetic conductors [5], etc. Among them, cross-dipole antenna is one of the most popular antennas for obtaining wideband CP radiation due to its excellent wideband operation characteristics. As a result, various cross-dipole antenna structures have been massively investigated to enhance the CP performance [6]–[17]. Recently, a vacant-quarter ring rotated feeding structure has attracted a lot of attention, and has been applied in CP antenna design due to its unique characteristic of 90° phase difference. In [6], a cross-dipole loaded with strip-line was used to achieve 15.6% CP bandwidth. Based on this configuration, several wideband CP antennas with parasitic elements are designed in [7]–[13], for example, parasitic loop resonators (28.6%) [2], parasitic magneto-electric dipoles (26.8%) [8], parasitic rotated-circular dipoles (47.8%) [9], a parasitic asymmetrical dipoles (53.4%) [10], a dual-square cavity ground (66.7%) [11], four parasitic triangle-patches [12], and four shorted coupled pads [13].

Apart from these parasitic strips, planar modified cross-dipoles [14]–[19] are also a potential means for obtaining broad CP performance. In [14], by introducing rectangular planar crossed dipoles, a wideband CP antenna with 24% CP bandwidth was obtained. Similarly, an elliptical cross-dipole patch, an asymmetric bowtie cross-dipole patch, a slit-loaded rectangular slot patch, a stepped rectangular patch and a L-shaped patch in [15]–[19] were employed to obtain

The associate editor coordinating the review of this manuscript and approving it for publication was Shah Nawaz Burokur.

wideband 3-dB axial ratio bandwidth (ARBW) of 96.6%, 51%, 23.2%, 55.1% and 67.5% respectively. Recently, some works show that the CP performance of antenna can also be further improved by introducing parasitic elements on the planar modified cross-dipoles [20]–[25]. By combining a bowtie-shaped parasitic patch with bowtie cross-dipoles [20], a CP antenna with 58.6% 3-dB ARBW can be realized. Correspondingly, a parasitic patch was etched on half ellipse cross-dipoles [21], achieves 68.6% 3-dB ARBW. A crossed-stepped-dipole loaded with a parasitic cross-slotted square patch, a crossed-slot-dipole with four bowtie-patches, a driven crossed-strip-dipole with two kinds of parasitic elements and a trapezoidal-cross-dipole with identical elements (horizontal and vertical part) are designed in [22]–[25], because these parasitic structures can generate additional CP mode, these CP antennas can realize 59.1%, 90.9%, 66% and 63.4% 3-dB ARBW respectively.

In this paper, we proposed a new broadband CP crossed dipole antenna with multiple modes. The antenna is composed of two pairs of cross-strip dipoles as driven elements, four square-slot patches, and four corner-truncated patches as parasitic elements. vacant-quarter rings are used as sequential phase feed-structure to generate a CP mode, which connect to crossed strip dipoles. By using these coupled rotated elements, multiple CP modes can be stimulated to satisfy the need of broadband CP radiation. In addition, four shorted square metal columns are also introduced in the antenna design to generate an additional CP resonance. A verified prototype was fabricated and measured in this paper. The tested results demonstrate the presented antenna features broadband CP performance with a wide impedance bandwidth (IBW) of 97.1% (0.90-2.60 GHz) and a broad axial-ratio bandwidth (ARBW) of 91.4% (0.95-2.55 GHz). Due to the compact structure and wideband bandwidth CP performance, the presented antenna might be suitable in modern communication systems for CP applications, for example, the GPS systems (L1 1.575 GHz) and WiBro systems (2.3-2.39 GHz).

II. ANTENNA DESIGN

A. ANTENNA CONFIGURATION

The geometry of the presented CP cross-dipole antenna is depicted in Fig. 1. The antenna is composed of two pairs of crossed strip dipoles (L3×W3) as driven elements, four outer parasitic elements (L1×L1) loaded with a tilted slot (L5×W5), and four inner parasitic elements (L2×L2) with truncated corner (W2×W2), which are arranged perpendicular to each other. vacant-quarter rings [1]–[20] are designed to connect the cross-strip dipoles as feeding structure, due to the ring length of $\lambda g/4$ providing a 90° phase difference between adjacent dipoles, which can stimulate CP radiation wave. R0 and R1 represent the values of inner and outer radiuses, respectively. It is noticed that the outer parasitic elements are connected to the end of driven crossed strip dipoles by a coplanar waveguide feeding structure, while the inner parasitic elements are placed at the edge of driven cross-strip dipoles by a capacitively coupled way. Meanwhile, these parasitic elements, driven elements and vacant-quarter rings are together printed on both side of an FR4-epoxy dielectric substrate ($\varepsilon r = 4.4$ and $\tan\delta = 0.02$), one of which is symmetric about the origin of the coordinates. Moreover, a square ground plane (L×L) is employed to solder 50-coaxial cable as a reflector with the height of H1 to achieve a directional radiation pattern. The optimized dimensional parameters of the presented antenna are listed in Table 1.

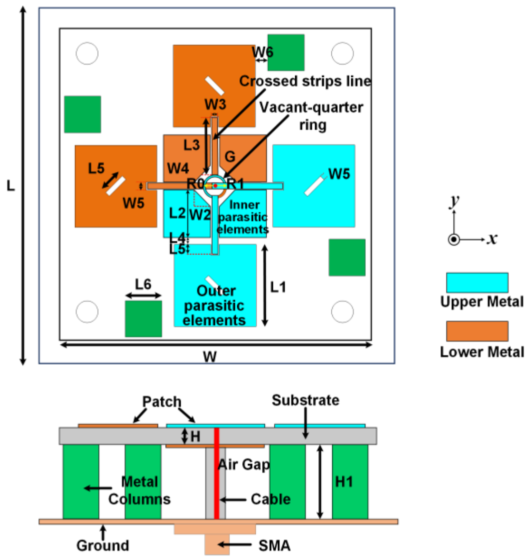

FIGURE 1. The geometry of the proposed antenna.

TABLE 1. The geometrical parameters of the proposed antenna.

Parameters	Values	Parameters	Values
L	148 mm	W	130 mm
L1	34 mm	W1	3.4 mm
L2	19.8 mm	W2	7.2 mm
L3	19.3 mm	W3	2.7 mm
L4	2.94 mm	W4	3.1 mm
L5	9.6 mm	W5	2.0 mm
L6	15 mm	W6	5.2 mm
R0	4.8 mm	R1	5.32 mm
H	0.8 mm	H1	36.6 mm

B. ANTENNA MECHANISM

In this section, an evolution of the presented antenna is shown to demonstrate the bandwidth enhancement mechanism in Fig. 2. Four antenna prototypes are proposed: Ant. 1: a common cross-dipole; Ant. 2: a cross-dipole with outer parasitic square elements loaded with tilted slot; Ant. 3: introducing inner square parasitic elements based on Ant. 2; Ant. 4: Ant. 3 with four shorted square metal columns. Fig. 3(a) and Fig. 3(b) show the corresponding simulated |S11| and AR results, respectively. Firstly, we can see that the Ant. 1 has a narrow circularly polarized bandwidth (CPBW) due to this usually structure in [1]–[20]. Secondly, by introducing parasitic square elements loaded with tilted slot into Ant. 2, a new

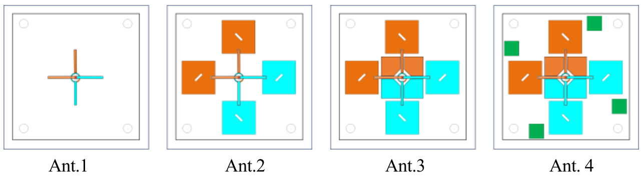

FIGURE 2. Four antenna structures in the design process.

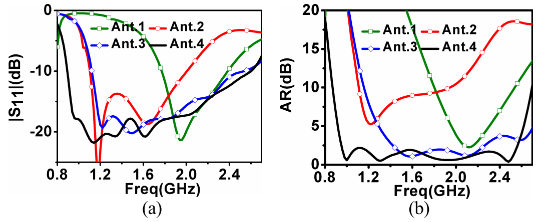

FIGURE 3. $|S_{11}|$ and AR curves for different antennas, (a) $|S_{11}|$ curves (b) AR curves.

AR resonance point is excited at 1.2 GHz, and the whole CPBW of Ant. 2 shifts towards low frequency. However, it needs to point out that the CPBW performance of Ant. 2 is poor and not satisfied with the need of application. To further enhance the CP performance and broaden the CPBW, four square parasitic elements are inserted to the Ant. 2, the IBW and ARBW of the Ant. 3 is significantly improved, and another AR resonance point is stimulated at 2.6 GHz. Eventually, Ant. 4 with four shorted square metal columns is designed to realize a broadband CP radiation. It is noticed that the CPBW is greatly enhanced to 91.4% (0.95-2.55 GHz). This is because that the combination of shorted square metal columns with outer parasitic square elements can be regarded as electric-magnetic dipoles, which can generate a new AR resonance point at 1 GHz. As a consequence, the antenna realizes a broad 3-dB ARBW of 91.4% (0.95-2.55 GHz) and a wide -10-dB IBW of 97.1% (0.90-2.60 GHz).

To illustrate the CP operation mechanisms of the presented antenna, the simulated surface current distributions on Ant. 1-Ant.4 at different frequency point and time phases are depicted in Fig. 4(a)-Fig. (d), respectively. At 1 GHz, the simulated current distributions mainly concentrate on the outer parasitic elements and four shorted square metal columns, and this distribution is similar to the shorted parasitic elements in [25]. Therefore, the combining four short square metal columns with outer parasitic elements can be regarded as a pair of crossed electric-magnetic dipoles, which can realize wider CP radiation, and radiate left-hand circularly polarized (LHCP) waves at same frequency with different time phases. It is observed that surface current distributions of Ant. 1-3 are mainly concentrated on cross-dipoles, outer parasitic elements and inner parasitic elements at 2.1 GHz, 1.2 GHz and 2.6 GHz, respectively, which are good consistent with the results of evolution of the antenna. In Fig. 4(a)-4(d), it can be observed that the surface current directions are clockwise with different time phases, and orthogonal in 0° and 90°. Thus, the presented antenna can excite LHCP waves at 1 GHz, 1.2 GHz, 2.1 GHz and 2.5 GHz.

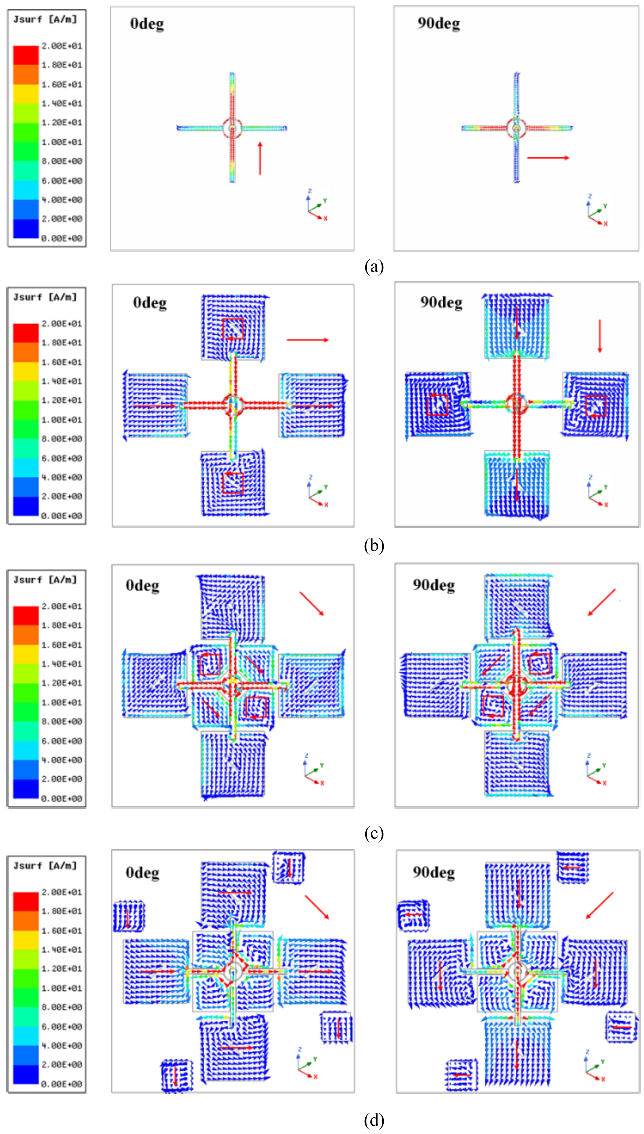

FIGURE 4. Simulated current distributions on the Ant. 1-4 with the phases of 0° and 90° at (a) 2.1 GHz, (b) 1.2 GHz (c) 2.6 GHz and (d) 1 GHz, respectively.

C. ANTENNA PARAMETER ANALYSIS

Fig. 5 shows the change of IBWs and ARBWs with different lengths of the outer parasitic elements (L1), inner parasitic elements (L2), crossed strip dipoles (L3) and shorted square metal columns (L6). It is observed that the parameters L1 and L2 have obviously impact on ARBWs in high frequency. However, the parameters L3 and L6 have influence on IBWs and ARBWs in low frequency and middle frequency, this is because that the crossed strip dipoles and shorted square metal columns generate resonant point at 1.3 GHz and 1.0 GHz. These are consistent with the surface current distributions in Fig. 4. Moreover, in order to illustrate the proposed antenna has an excellent performance, a distinct comparison between the previous cross-dipole CP antenna and presented CP antenna is plotted in Table 2.

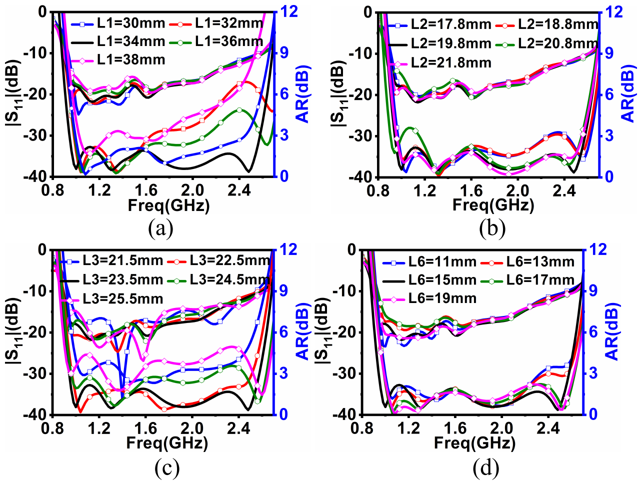

FIGURE 5. AR of the proposed antenna with different parameters: (a) L1, (b) L2, (c) L3 and (d) L6.

TABLE 2. Comparison of the proposed antenna to previous presented antenna.

Ref. Antenna	Size (λ_0)	-10 dB IBW (%)	3-dB ARBW (%)	CP-BW (%)	Average Gain (dBic)
[7]	1.05×1.05 ×0.24	38.2	28.6	28.6	8.0
[8]	0.64 ×0.64 ×0.16	59.8	26.8	26.8	8.0
[9]	0.4 ×0.4 ×0.17	66.2	41.3	41.3	6.0
[10]	1.1 ×1.1×0.28	67.5	53.4	49.4	8.0
[11]	0.57 ×0.57 ×0.24	79.4	66.7	66.7	6.5
[12]	0.59 ×0.59 ×0.24	53.3	58.9	53.3	8.0
[13]	1.17 ×1.17 ×0.29	95.0	85.5	85.5	5.4
[14]	0.45 ×0.45 ×0.24	50.2	27	27	6.2
[15]	0.88 ×0.88 ×0.23	57	51	51	9.6
[17]	0.44 ×0.44 ×0.15	31.6	23.2	23.2	7.25
[18]	2.06 ×2.06 ×0.13	66.9	55.1	55.1	10
[19]	1.81 ×1.81 ×0.23	92.8	67.5	67.5	11.2
[20]	0.79 ×0.79 ×0.27	68.9	58.6	58.6	8.2
[23]	1.1 ×1.1 ×0.4	93.1	90.9	86.5	4.5
[24]	1.04×1.04×0.26	77.6	66	66	7.2
[25]	0.46 ×0.46 ×0.1	78.3	63.4	63.4	4.2
Proposed	**1.04×1.04×0.26**	**95.5**	**94.4**	**93**	**6.8**

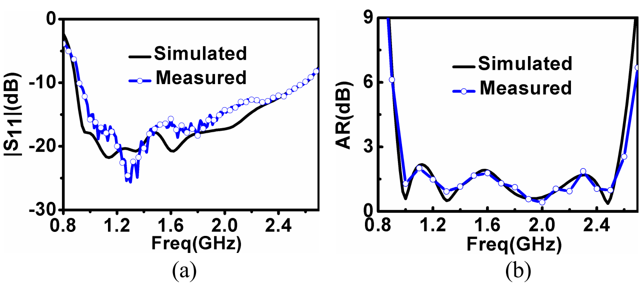

FIGURE 6. and measured $|S_{11}|$ and AR results of the antenna.

III. EXPERIMENTAL RESULTS

The presented broadband CP cross-dipole antenna was fabricated, and measured to validate the accuracy of the optimized design. The comparison of the simulated and measured |S11| and AR are shown in Fig. 6. It can be known that the

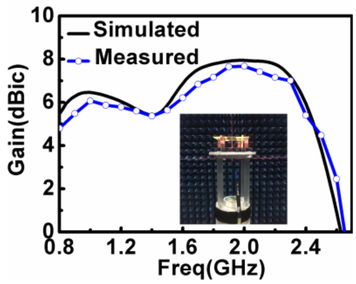

FIGURE 7. Simulated and measured antenna gains and measurement photograph.

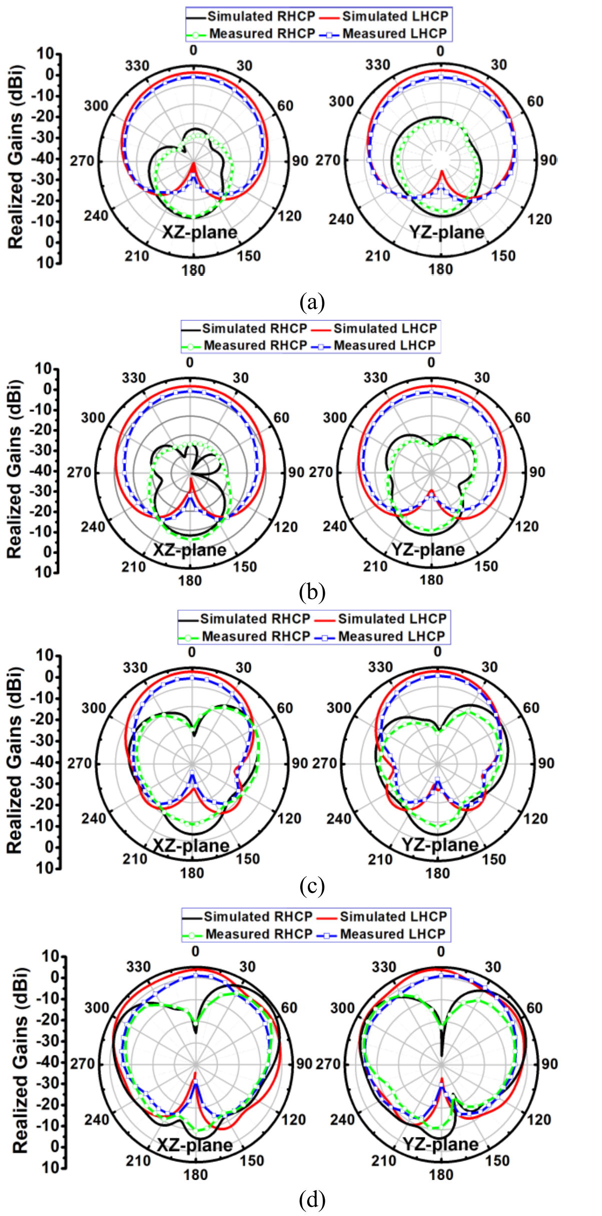

FIGURE 8. Simulated and measured antenna radiation patterns at (a) 1.0 GHz, (b) 1.3 GHz, (c) 1.9 GHz and (d) 2.5 GHz.

simulated |S11| and AR are 97.1% (0.90-2.60 GHz) and 91.4% (0.95-2.55 GHz), respectively. However, the measured |S11| and AR are 95.5% (0.92-2.60 GHz) and

94.4% (0.95-2.65 GHz), respectively. The measured results slightly shift towards high frequency compared with simulated results due to fabrication and measurement errors. Fig. 7 depicts the simulated and measured broadside gain, and the average gain is about 6.8 dBic within the CPBW. In addition, Fig. 8(a)-8(d) plots the simulated and measured unidirectional radiation patterns at 1, 1.3, 1.9, and 2.5 GHz, respectively. It is noted that the stable patterns can be obtained through whole operating bandwidth, and the LHCP radiation patterns can be seen as expected.

IV. CONLUSIONS

In this paper, a broadband crossed dipole CP antenna with multiple modes is proposed. The antenna is composed of two pairs of cross-strip dipoles as driven elements, four square-slot patches, and four corner-truncated patches as parasitic elements. A pair of vacant-quarter printed rings is used as sequential phase feeding structure to generate a CP mode, which connect to crossed strip dipoles. By using these coupled rotated elements, multiple CP modes can be stimulated to satisfy the need of broadband CP radiation. In addition, four shorted square metal columns are also introduced in the antenna design to excite an additional CP resonance. A verified prototype was fabricated and measured in this paper. The measured results demonstrate the designed antenna features broadband CP performance with a wide IBW of 95.5% (0.92-2.60 GHz), and a broad ARBW of 94.4% (0.95-2.65 GHz). Due to the compact structure and wideband bandwidth CP performance, the proposed antenna might be suitable in modern communication systems for CP applications, for example, the GPS systems (L1 1.575 GHz) and WiBro systems (2.3-2.39 GHz).

REFERENCES

[1] G. Varshney, V. S. Pandey, R. S. Yaduvanshi, and L. Kumar, "Wide band circularly polarized dielectric resonator antenna with stair-shaped slot excitation," *IEEE Trans. Antennas Propag.*, vol. 65, no. 3, pp. 1380–1383, Mar. 2017.

[2] S. Fakhte, H. Oraizi, R. Karimian, and R. Fakhte, "A new wideband circularly polarized stair-shaped dielectric resonator antenna," *IEEE Trans. Antennas Propag.*, vol. 63, no. 4, pp. 1828–1832, Apr. 2015.

[3] E. H. Lim, K. W. Leung, and X. S. Fang, "The compact circularly-polarized hollow rectangular dielectric resonator antenna with an underlaid quadrature coupler," *IEEE Trans. Antennas Propag.*, vol. 59, no. 1, pp. 288–293, Jan. 2011.

[4] K. X. Wang and H. Wong, "A wideband millimeter-wave circularly polarized antenna with 3-D printed polarizer," *IEEE Trans. Antennas Propag.*, vol. 65, no. 3, pp. 1038–1046, Mar. 2017.

[5] K. Agarwal, Nasimuddin, and A. Alphones, "Wideband circularly polarized AMC reflector backed aperture antenna," *IEEE Trans. Antennas Propag.*, vol. 61, no. 3, pp. 1456–1461, Mar. 2013.

[6] J.-W. Baik, K.-J. Lee, W.-S. Yoon, T.-H. Lee, and Y.-S. Kim, "Circularly polarised printed crossed dipole antennas with broadband axial ratio," *Electron. Lett.*, vol. 44, no. 13, pp. 785–786, 2008.

[7] J. W. Baik, T. H. Lee, S. Pyo, S. M. Han, J. Jeong, and Y. S. Kim, "Broadband circularly polarized crossed dipole with parasitic loop resonators nd its arrays," *IEEE Trans. Antennas Propag.*, vol. 59, no. 1, pp. 80–88, Jan. 2011.

[8] S. X. Ta and I. Park, "Crossed dipole loaded with magneto-electric dipole for wideband and wide-beam circularly polarized radiation," *IEEE Antennas Wireless Propag. Lett.*, vol. 14, pp. 358–361, 2015.

[9] R. Xu, J.-Y. Li, and W. Kun, "A broadband circularly polarized crossed-dipole antenna," *IEEE Trans. Antennas Propag.*, vol. 64, no. 10, pp. 4509–4513, Oct. 2016.

[10] G. Feng, L. Chen, X. Xue, and X. Shi, "Broadband circularly polarized crossed-dipole antenna with a single asymmetrical cross-loop," *IEEE Antennas Wireless Propag. Lett.*, vol. 16, pp. 3184–3187, 2017.

[11] Nguyen, Truong Khang, H. H. Tran, and N. Nguyen-Trong, "A wideband dual-cavity-backed circularly polarized crossed dipole antenna," *IEEE Antennas Wireless Propag. Lett.*, vol. 16, pp. 3135–3138, 2017.

[12] H. H. Tran, N. Nguyen-Trong, T. K. Nguyen, and A. M. Abbosh, "Bandwidth enhancement utilizing bias circuit as parasitic elements in a reconfigurable circularly polarized antenna," *IEEE Antennas Wireless Propag. Lett.*, vol. 17, no. 8, pp. 1533–1537, Aug. 2018.

[13] Z. Zhao, Y. Li, L. Wang, Z. Tang, and Y. Yin, "Design of broadband circularly polarized antenna via loading coupled rotated dipoles," *Microw. Opt. Technol. Lett.*, vol. 61, no. 2, pp. 425–430, Feb. 2019.

[14] Y. He, W. He, and H. Wong, "A wideband circularly polarized cross-dipole antenna," *IEEE Antennas Wireless Propag. Lett.*, vol. 13, pp. 67–70, 2014.

[15] L. Zhang, S. Gao, Q. Luo, P. R. Young, Q. Li, Y.-L. Geng, and R. A. Abd-Alhameed, "Single-feed ultra-wideband circularly polarized antenna with enhanced Front-to-Back ratio," *IEEE Trans. Antennas Propag.*, vol. 64, no. 1, pp. 355–360, Jan. 2016.

[16] H. H. Tran and I. Park, "Wideband circularly polarized cavity-backed asymmetric crossed bowtie dipole antenna," *IEEE Antennas Wireless Propag. Lett.*, vol. 15, pp. 358–361, 2016.

[17] Q. Chen, H. Zhang, L.-C. Yang, and T. Zhong, "A metasurface-based slit-loaded wideband circularly polarized crossed dipole antenna," *Int. J. RF Microw. Comput.-Aided Eng.*, vol. 28, no. 1, Jan. 2018, Art. no. e21173.

[18] W. Yang, Y. Pan, S. Zheng, and P. Hu, "A low-profile wideband circularly polarized crossed-dipole antenna," *IEEE Antennas Wireless Propag. Lett.*, vol. 16, pp. 2126–2129, 2017.

[19] X. Liang, J. Ren, L. Zhang, C. He, J. Geng, W. Zhu, and R. Jin, "Wideband circularly polarized antenna with dual-mode operation," *IEEE Antennas Wireless Propag. Lett.*, vol. 18, no. 4, pp. 767–770, Apr. 2019.

[20] H. H. Tran, I. Park, and T. K. Nguyen, "Circularly polarized bandwidth-enhanced crossed dipole antenna with a simple single parasitic element," *IEEE Antennas Wireless Propag. Lett.*, vol. 16, pp. 1776–1779, 2017.

[21] Z. Guo, Z. Zhao, Y. Yang, and X. Ding, "A directional circularly polarized crossed-dipole antenna with bandwidth enhancement," *Microw. Opt. Technol. Lett.*, vol. 60, no. 9, pp. 2161–2167, Sep. 2018.

[22] G. Feng, L. Chen, X. Xue, N. Li, and X. Shi, "Broadband CP crossed-stepped-dipole antenna incorporating a cross slotted square patch," *IET Microw., Antennas Propag.*, vol. 13, no. 3, pp. 340–345, Feb. 2019.

[23] G. Feng, L. Chen, X. Wang, X. Xue, and X. Shi, "Broadband circularly polarized crossed bowtie dipole antenna loaded with parasitic elements," *IEEE Antennas Wireless Propag. Lett.*, vol. 17, no. 1, pp. 114–117, Jan. 2018.

[24] L. Wang, W.-X. Fang, Y.-F. En, Y. Huang, W.-H. Shao, and B. Yao, "Wideband circularly polarized cross-dipole antenna with parasitic elements," *IEEE Access*, vol. 7, pp. 35097–35102, 2019.

[25] W. J. Yang, Y. M. Pan, and S. Y. Zheng, "A low-profile wideband circularly polarized crossed-dipole antenna with wide axial-ratio and gain beamwidths," *IEEE Trans. Antennas Propag.*, vol. 66, no. 7, pp. 3346–3353, Jul. 2018.

LEI WANG was born in Shaanxi, China, in 1991. He received the B.S. and M.S. degrees in electromagnetic field and microwave technology from Xidian University, Xian, China, in 2017. After that, he joined the China Electronic Product Reliability and Environmental Testing Research Institute (CEPREI), Guangzhou, China, and has severed as an Engineer. His research interests include electromagnetic compatibility and design of circularly polarized microstrip antennas.

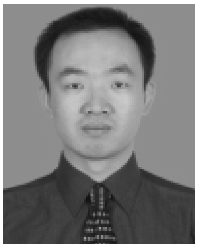

WEN-XIAO FANG received the B.S., M.S., and Ph.D. degrees in condensed-matter physics from Sun Yat-sen University, Guangzhou, China, in 2002, 2005, and 2008, respectively. He was a Visiting Scholar with the Hong Kong University of Science and Technology, Hong Kong, in 2009. After that, he joined the China Electronic Product Reliability and Environmental Testing Research Institute (CEPREI), and has been severed as a Senior Engineer of the Science and Technology on Reliability Physics, since 2011. His current interests include the electromagnetic compatibility in integrated circuit and component level, and electromagnetism application in power electronics.

WEI-HENG SHAO was born in Panjin, Liaoning, in 1989. He received the B.Eng. and M.Eng. degrees in electrical engineering from Northeastern University, Shenyang, China, in 2012 and 2014, respectively. Since 2014, he has been with the China Electronic Product Reliability and Environmental Testing Research Institute (CEPREI). His current interests are the electromagnetic compatibility in integrated circuits, component level, and system level.

BIN YAO was born in Neijiang, Sichuan, in 1980. He received the B.S. degree in applied chemistry and the M.S. degree in material science from the University of Electronic Science and Technology of China (UESTC), in 2003 and 2006, respectively. He is currently a Senior Engineer with the China Electronic Product Reliability and Environmental Testing Research Institute (CEPREI). His current research interests include reliability evaluation and failure analysis of electronic products.

YUN HUANG was born in Sichuan, China, in 1970. He received the M.S. degree in microelectronic technology from the University of Electronic Science and Technology of China (UESTC), in 1998. Since 1998, he has been a Research Engineer and a Professor with the China Electronic Product Reliability and Environmental Testing Research Institute (CEPREI), where he was involved in more than tens of projects in electromagnetic compatibility, microelectronics, and RF devices reliability.

YUN-FEI EN received the B.S. degree in semiconductor physics and solid state electronics, the M.S. degree in semiconductor devices and microelectronics, and the Ph.D. degree from Xidian University, in 1990, 1995, and 2013, respectively. Since 1995, she has been with the China Electronic Product Reliability and Environmental Testing Research Institute (CEPREI). She worked on the failure mechanism and reliability evaluation of components. Since 2006, she has been serving as a Research Fellow of the Science and Technology on Reliability Physics and Application of Electronic Component Laboratory. She is the author or coauthor of five books and more than 40 scientific publications in journals and international conferences. Her research interests include electromagnetic compatibility, microelectronics, and failure analysis of electronic components.